EA4EPQ REE&PQJ

Renewable Energy, Environment, and Power Quality Journal (REE&PQJ)
ISSN:3020-531X
Volume 26, July 2026

Performance analysis of Savonius rotors with straight and Bach-type twisted blades

Velásquez L[1], Chica E[1], Rubio-Clemente A[1,2]

[1]Grupo de Investigación Energía Alternativa, Facultad de Ingeniería, Universidad de Antioquia UdeA, Calle 70, No. 52-21, Medellín, Colombia.

[2]Escuela Ambiental, Facultad de Ingeniería, Universidad de Antioquia UdeA, Calle 70, No. 52-21, Medellín, Colombia.

Phone/Fax number: +57 604 2195547, e-mail: ainhoa.rubioc@udea.edu.co

Abstract. In this work, experimental comparisons are conducted when two Savonius-type vertical-axis wind turbine rotors of different blade twist angles (γ) are placed with the same aspect ratio (AR = 2.0). During the initial setup, a straight blade (γ=0°) was used in the first design; while in the second configuration, twisted blades were employed with a γ of 30°. The rotors were checked for aerodynamic performance in comparable wind tunnel configurations along with the power coefficient (C_p), the starting torque and the rotational stability. The rotor at a blade γ value of 30° reached a C_p equal to 0.232 compared to the straight-blade rotor (C_p = 0.165). The torque variation with less variability and self-starting ability was observed in the twisted blade setup, which was attributable to a better flow interface of the advancing and return blades. Results demonstrated that a moderate blade twist for the system can improve the aerodynamic efficiency of the Savonius rotors without a significant modification of the production complexity. Thus, the configuration conformed by a γ and an AR of 30° and 2.0, respectively, presented an optimal blend between performance and simplicity, which made it suitable for small-scale power generation under low-wind conditions.

Key words. Wind turbine, Savonius rotor, blade twist angle, aspect ratio, experimental study, aerodynamic performance.

1. Introduction

The global transition to sustainable energy systems is an urgent and required necessity due to the increasing climate emergency and the requirement to cut back on the burning of fossil fuels [1, 2]. In this framework, wind power is important for its low environmental impact, scalability and for possible integration with centralized or distributed power systems. Nevertheless, considering that it can be fully exploited locally, in urban and rural regions with low wind speeds, technologies must be adapted for such cases.

In recent years, vertical-axis wind turbines (VAWTs) have gained increasing attention as a complementary alternative to conventional horizontal-axis wind turbines (HAWTs). While HAWTs generally achieve higher efficiencies under steady and high-speed wind conditions, VAWTs offer several advantages. Among these benefits, VAWTs can operate independently on wind direction, produce less noise, and require simpler maintenance. Additionally, they can be installed closer to the ground. Consequently, these capabilities allow them to be implemented in urban environments, decentralized contexts, and municipal-scale renewable energy initiatives that support the ongoing energy transition [3, 4].

Among all VAWT combinations, Savonius rotor is relatively simple in terms of structure, easy in fabrication and very good at auto-starting for wind operation. However, its major drawback is the relatively low aerodynamic efficiency, which drives extensive studies in its aerodynamics to optimize its performance, including geometric optimization. In previous works, factors, such as the blade twist angle (γ) and the aspect ratio (AR), directly affect the power coefficient (C□), the torque uniformity and, in general, the operating stability [3,4].

Anbarsooz et al. reported some improvements in torque smoothness as γ was increased, but only a minor decrease in C□ was reported [5]. In contrast, Zadeh et al. and Damak et al. demonstrated that modest helical/twisted configurations substantially enhanced performance with C□ values around 0.20 [6, 7]. Similarly, Jeon et al. and Kamoji et al. mentioned the importance of AR for structural stability and aerodynamics and, therefore, balanced geometrical design is a key factor in the performance of the technology [8, 9].

Despite these innovations, previous studies mainly used numerical simulations or small experimental datasets, which have often been restricted to narrow geometric ranges. Thus, there is still an urgent need for systematic experimental procedures that can support the verification of real aerodynamic behavior for the practical, high-performance design combining efficiency, manufacturability, and robustness, among other aspects.

In this context, the present study aims to experimentally evaluate and compare the performance of two Savonius rotors with different blade twist angles (γ = 0° and 30°) and a constant aspect ratio (AR = 2.0). In this research, the blade twist effect on aerodynamic efficiency is analyzed under several operational characteristics through controlled wind tunnel tests. The response variable is the power coefficient (C□). This study is based on empirical data, which will facilitate the design of optimized Savonius turbines for small-scale wind energy generation and support the sustainable energy transition of existing research work.

2. Materials and methods

2.1. Geometric configuration of the rotors

To compare the aerodynamic aspects of the blade twist, two versions of Savonius VAWTs were selected. The dimensions of the two rotors are similar. Then the diameter (D) of about 0.4 m was used. This dimension was mostly chosen based on the maximum printable volume of the 3D printing equipment, allowing the blades to be manufactured as single pieces to ensure structural stability and surface continuity (for details in geometry fabrication, see Section 2.2). AR — defined as H/D — was 2.0, resulting in rotor height (H) of 0.8 m, and the value of AR was selected because Velásquez et al. considered this AR to be almost optimum for the gain of Cp in Savonius rotors [10]. Additionally, the reference model contained straight blades (γ = 0°) and the second configuration included a Bach-type twist (γ = 30°).

Each rotor was made up of two semi-cylindrical blades and a central shaft, supported by circular end plates of 5 mm thickness. The twisted blade was made by applying a uniform helical deformation along the rotor height to form a smooth turning profile of the blade from the top to the bottom of the rotor. The geometry provides a better aerodynamic interaction and potential for increased torque stability and self-starting of the blade progression and return.

The geometry of Bach-type profiles corresponded with the dimensional relationships initially proposed by Bach and further refined by Kamoji et al. and Gallo et al. [11, 12] to set the flow separation and pressure distribution. All critical dimensions were scaled to the necessary curvature and overlap parameters in the geometric ratios used to estimate blade curvature, computed by the rotor diameter (D) as O = 0.968D, P = 0.174D, and Q = 0.094D. The two rotor configurations considered in this work are shown in Figure 1.

2.2. Rotor fabrication via 3D printing

The turbine models were created using an additive manufacturing process on the Creality CR-M4 3D printer. The equipment was selected based on its large build volume and high dimensional precision. Additionally, it was suited for the manufacture of full-scale rotors being evaluated. 3D printing made it possible to achieve geometric precision, reproducibility, and the ability to fabricate more complex blade shapes than are possible with standard milling. This polymer has good mechanical strength, impact resistance, and thermal stability, making it hard enough to withstand aerodynamic testing, but flexible enough to prevent cracking while in use. Polyethylene terephthalate glycol (PETG) has outstanding bonding property and excellent layer adhesion and surface finish which reduce post-processing and lead to smooth aerodynamic surfaces.

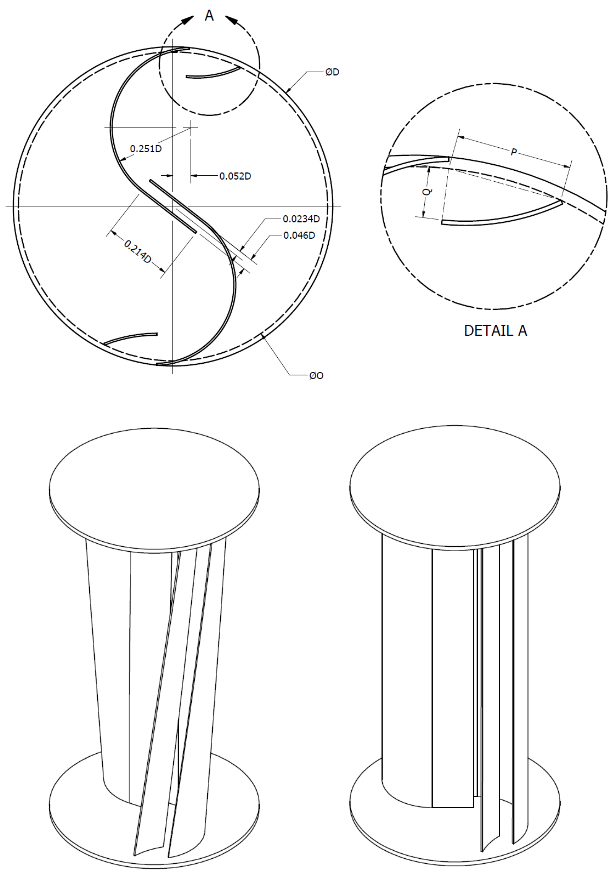

a) b)

Fig. 1. Savonius rotor designs with Bach-type profiles under different blade twist angles. (a) Twisted and (b) Straight blades.

The rotor parts were printed in accordance with the same manufacturer standard for the production conditions specified to ensure standardized quality between these models. The nozzle temperature was 220 °C, the print bed was kept at 70 °C, the layer height was maintained at 0.2 mm. The print speed was constant at 150 mm/s and infill density kept at 100% in order to obtain complete structural stability. To achieve an accurate reproduction of the blade curvature, parts were printed using a 0.4 mm nozzle with a printing accuracy of ±0.1 mm. For the assembly of each rotor component and securing the axial alignment, two separate sections were fabricated. The first section was made up of blades and the lower end plate, and the second part was the upper end plate with guide slots to fit the first part. As expected, the printed rotors with consistent surface texture showed high geometric fidelity relative to the CAD design. With a single printer model and constant manipulation of the parameter input throughout this process, production variability was low, and test effects could be interpreted via geometric variations of the rotor designs.

High numerical precision was provided for the geometric ratios (O, P, Q) but the actual manufacturing was subject to a 3D printing tolerance. Such a deviation results in a relative error of 0.025% in relation to the rotor diameter, which is considered negligible in the aerodynamic characterization of drag-driven turbines at this scale. Furthermore, the inherent robustness of the Savonius design suggests that these minor manufacturing variances do not significantly compromise performance, confirming its suitability for low-cost and small-scale applications [13].

2.3. Experimental setup

The investigation was conducted in a wind tunnel (Figure 2). The tunnel runs on an open-circuit design with axial airflow powered by an industrial-grade Soler & Palau TGT/6-1000-9/26-B-7 1/2 HP fan. Its test section has a square cross-section of 0.8 m × 0.8 m and is 1.2 m long. In this regard, wide space and low blockage effects for the installation of the turbine models were provided. In the configuration tested, the blockage ratio varied between 4 and 13%, and while this figure is acceptable with regard to comparative aerodynamic measurements, no blockage correction was performed on the recorded data. Rotors in the system were mounted vertically on a rigid aluminum frame, which was arranged to maintain a coaxial alignment of the shaft with the free-stream velocity vector. The mechanical torque produced by the turbine was transmitted through a precision coupling to a Futek TRS 605-FSH02052 rotary torque transducer with an integrated optical encoder. The torque sensor has a nominal range of 0–1 N·m, which yields simultaneous torque and rotational speed measurements at a resolution of 0.001 N·m and ±0.1 rpm, respectively. A 6 V DC motor was mounted downstream of the sensor to act as a controllable electrical load. The motor was driven from the DC supply (0–30 V, 0–10 A), controlled by altering the input voltage and the current for brake torque response. This setup enables simulations of multiple operating conditions and accurate calculation of overall torque–speed–power curves per rotor.

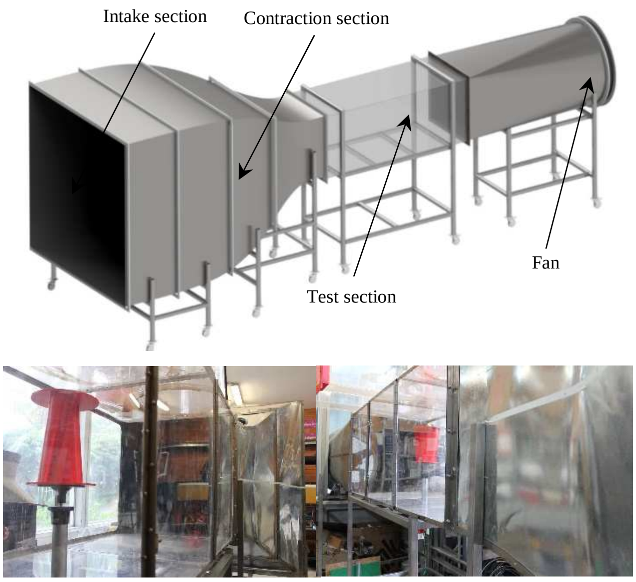

Fig. 2. Principal wind tunnel sections and photographic views.

The free-stream wind flow speed at the mid-plane of the rotor was measured with a 20 mm impeller bearing Flowatch anemometer with an accuracy of ±2%. The anemometer was positioned 50 mm upstream of the rotor axis to minimize flow disturbance. All analogy signals (torque, angular velocity, and voltage) were recorded continuously with a data acquisition system. This configuration provided fast visualization of aerodynamic performance, combined with the simultaneous acquisition of torque and speed information.

The instantaneous mechanical output power ($P_{ou□}$) of the turbine was obtained from the measured torque (T) and corresponding angular velocity (ω), shown by Eq. (1).

$$\boldsymbol{P}_{\text{ou}} = \boldsymbol{T} \times \boldsymbol{\omega} \quad (1)$$

where T is expressed in newton-meters (N·m) and ω, in radians per second (rad/s).

The available kinetic power of the wind (P_{wind}) through the rotor swept area was calculated according to Eq. (2).

$$\mathbf{P_{wind}} = \frac{1}{2}\boldsymbol{\rho} \times \mathbf{A} \times \mathbf{V}^3 \quad (2)$$

where ρ is air density (kg/m³), A is swept area of the turbine (m²), and V is free-stream wind velocity (m/s). For this study, an air density of ρ = 1.225 kg/m³ was assumed, corresponding to standard atmospheric conditions at 25 °C and 1 atm. For VAWTs, A is defined as the product of the rotor diameter (D) and its height (H), as the turbine interacts with the wind across a cylindrical section, as shown in Eq. (3).

$$\mathbf{A} = \mathbf{D} \times \mathbf{H} = \mathbf{0.4\,m} \times \mathbf{0.8\,m} = \mathbf{0.32\,m^2} \quad (3)$$

The efficiency of the rotors was calculated using the dimensionless C□, which expresses the ratio of the mechanical power extracted by the turbine to the total power available, as defined in Eq. (4).

$$\mathbf{C} = \frac{\mathbf{P_{ou}}}{\mathbf{P_{wind}}} = \frac{(\mathbf{T} \times \boldsymbol{\omega})}{(½ \times \boldsymbol{\rho} \times \mathbf{A} \times \mathbf{V}^3)} \quad (4)$$

This parameter quantifies the fraction of the kinetic energy effectively converted into mechanical energy at the shaft. To further characterize the turbine operation, the tip speed ratio (TSR) was determined by using Eq. (5).

$$\mathbf{TSR} = \frac{(\boldsymbol{\omega} \times \mathbf{R})}{\boldsymbol{V}} \quad (5)$$

where R = D/2 represents the rotor radius. The TSR defines the relationship between the tangential velocity of the blade tip and the incident wind speed. This formulation is appropriate for VAWTs as the tangential velocity remains uniform for the entire blade span at a constant radius, serving as the fundamental non-dimensional parameter to correlate aerodynamic performance and flow field behavior [14-16].

The braking torque was varied on each test based on the electrical load applied to the DC motor in order to arrive at steady state for the turbine. The data were measured for 0.05 s after the rotating velocity had stabilized. To maintain the reproducibility of the data, three independent tests were carried out in each of the different operating conditions. This data has allowed a reliable comparison of the straight-blade and the Bach-type twisted-blade Savonius rotors in the same experimentation, based on their aerodynamic performance.

3. Results and discussion

The C_p, as a function of the TSR for the two rotors, is illustrated in Figure 3. Both cases present a trend typical of that for drag-type vertical-axis turbines; i.e., a rapid increase in C_p with TSR up to a maximum, followed by a gradual decrease as the aerodynamic drag takes over.

At a TSR of roughly 0.59, the straight-blade rotor (γ=0°) reached a maximum value of C_p 0.165, while the twisted Bach-type rotor (γ=30°) showed that a TSR of 0.69 gave a maximum value of 0.232 to the rotor. After a standard uncertainty analysis and considering the ±2% tolerance of the flow meter, the uncertainty in C_p is estimated to be approximately ±6% due to the cubic relationship between power and wind velocity (P≈V3). Hence, the maximum C_p values are calculated to be 0.233±0.014 and 0.165±0.010.

Figure 3 presents these experimental results with shaded areas, also known as uncertainty bands, in light grey and light red. Such continuous visualization technique was employed instead of the usual discrete error bars to achieve ease of visualization for the figure, to avoid visual saturation, and to be able to accurately measure the ranges of performance. Even with the experimental tolerance, the separation of the uncertainty bands verifies the efficiency enhancement is statistically significant, which corresponds to a relative increase of ~ 41% in the twisted configuration.

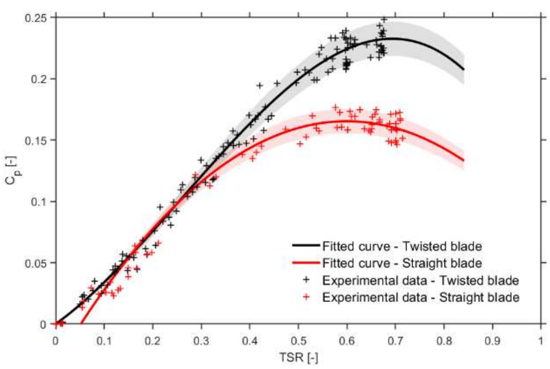

Fig. 3. Power coefficient (C_p) as a function of the tip speed ratio (TSR).

Both turbines exhibited a reduced C_p level. This can be attributed to greater drag forces and flow separation around the returning blade, at TSR values greater than 0.7. Such results are in accordance with the data of El-Askary et al. and Zakaria et al., who reported an enhanced torque stability and a higher efficiency in helically twisted Savonius designs [12, 17].

The rotor with γ = 30° was found to start rotation sooner and earlier than the straight-blade model in startup tests at low wind speeds (V < 5 m/s). Because the helical shape allows at least one blade section to be continuously exposed to the wind, this avoids dead zones and allows for motion from rest, which is particularly beneficial for small-scale power systems that require the use of variable or low-speed wind power.

The aerodynamic response toward the twisted rotor was better, which can be explained by the redistribution of the local flow field along the blade height. This progressive helical arrangement produces a joint drag–lift contribution, and some portion of the incoming kinetic energy in response can be converted by the aerodynamic behavior to useful torque. Therefore, it is not exclusively associated with resistance. This behavior is responsible for diminished recirculation zones in the overlap region between the blades and a relatively stable wake pattern downstream. Thanks to these developments, Bach-type twisted Savonius rotors could represent a plausible choice for urban, or off-grid uses where low noise and compactness, as well as excellent self-starting capability, are desirable traits.

4. Conclusion

In the laboratory tests on two Savonius rotor design forms, the effect of wind energy conversion on the blade twist in controlled testing condition was clearly compared. The 30° helical twist demonstrated a much larger aerodynamic performance and achieved a maximum C_p of 0.232 (compared to 0.165 for straight-blade rotor). This corresponds to an increase in efficiency of ~ 41%, further proving that the Bach-type twisted geometry can enhance the aerodynamic interaction between the advancing and returning blades, thus yielding smoother torque output and higher self-starting capacity.

Apart from the increased efficiency, the torques oscillated less with the helical configuration, which resulted in a more stable operation and a greater mechanical lifetime. These properties are beneficial for small and low wind-speed processes (self-starting and constant rotation rate) that depend on reliable energy production. Finally, a γ of 30° provided a good compromise among aerodynamic efficiency, toughness, and manufacturability in terms of design. The production of the rotor models with PETG filament using 3D printing verified the possibilities of additive manufacturing in rapid and accurate model generation of aerodynamic parts.

For the overall purpose, the results achieved show that the optimization by geometry can still be regarded as a good way to optimize efficiency for vertical-axis of Savonius-type wind turbines. The experimental findings proposed here provide a robust basis for further investigation on the combined influence of blade overlap ratio, number of stages, and leading-edge curvature with respect to further power density enhancement and larger applicability of these turbines in a decentralized field of renewable energy.

Acknowledgement

The authors gratefully acknowledge the financial support provided by the Colombian Ministry of Science, Technology, and Innovation “MinCiencias” through "Patrimonio Autónomo Fondo Nacional de Financiamiento para la Ciencia, la Tecnología y la Innovación, Francisco José de Caldas" (Perseo Alliance, Contract No. 112721-392-2023).

References

[1] Falcone, P. M. (2023). Sustainable energy policies in developing countries: a review of challenges and opportunities. Energies, 16(18), 6682.

[2] Murray, E. C., & Montgomery, H. (2025). The ‘climate emergency’, and how we respond. Future Healthcare Journal, 12(1), 100228.

[3] Salvador-Gutierrez, B., Sanchez-Cortez, L., Hinojosa-Manrique, M., Lozada-Pedraza, A., Ninaquispe-Soto, M., Montaño-Pisfil, J., & Vigo-Roldán, A. (2025). Vertical-Axis Wind Turbines in Emerging Energy Applications (1979–2025): Global Trends and Technological Gaps Revealed by a Bibliometric Analysis and Review. Energies, 18(14), 3810.

[4] Prajzendanc, P., & Kreischer, C. (2025). A review of new technologies in the design and application of wind turbine generators. Energies, 18(15), 4082.

[5] M. Anbarsooz, M. (2016). Aerodynamic performance of helical Savonius wind rotors with 30 and 45 twist angles: Experimental and numerical studies. Proceedings of the Institution of Mechanical Engineers, Part A: Journal of Power and Energy, 230, 6, 523–534.

[6] Zadeh, M. N., Pourfallah, M., Sabet, S. S., Gholinia, M., Mouloodi, S., & Ahangar, A.T. (2021). Performance assessment and optimization of a helical Savonius wind turbine by modifying the Bach’s section. *SN Applied Sciences*, 3 (8), 739.

[7] Damak, A., Driss, Z., & Abid, M.S. (2018). Optimization of the helical Savonius rotor through wind tunnel experiments. Journal of Wind Engineering and Industrial Aerodynamics, 174, 80–93.

[8] Jeon, S., Kim, B., & Huh, J. (2015). Comparison and verification of wake models in an onshore wind farm considering single wake condition of the 2 MW wind turbine. Energy, 93, 1769–1777.

[9] Kamoji, M. A., Kedare, S. B., & Prabhu S. V. (2009). Performance tests on helical Savonius rotors. Renewable Energy, 34(3), 521–529.

[10] Velásquez, L., Rengifo, J., Saldarriaga, A., Rubio-Clemente, A., & Chica, E. (2025). Geometric Optimization of Savonius Vertical-Axis Wind Turbines Using Full Factorial Design and Response Surface Methodology. Sci, 7(4), 154.

[11] Gallo, L. A., Chica, E. L., & Flórez, E.G. (2022). Numerical optimization of the blade profile of a Savonius type rotor using the response surface methodology. Sustainability, 14(9), 5596.

[12] El-Askary, W. A., Saad, A. S., AbdelSalam, A. M., & Sakr, I.M. (2018). Investigating the performance of a twisted modified Savonius rotor. Journal of Wind Engineering and Industrial Aerodynamics, 182, 344–355.

[13] Chitura, A. G., Mukumba, P., & Lethole, N. (2024). Enhancing the performance of Savonius wind turbines: a review of advances using multiple parameters. Energies, 17(15), 3708.

[14] Pouransari, Z., & Behzad, M. (2024). Numerical investigation of the aerodynamic performance of a hybrid Darrieus-Savonius wind turbine. Wind Engineering, 48(1), 3-14.

[15] Ghafoorian, F., Hosseini Rad, S., & Moghimi, M. (2025). Enhancing self-starting capability and efficiency of hybrid Darrieus–Savonius vertical axis wind turbines with a dual-shaft configuration. Machines, 13(2), 87.

[16] Marchewka, E., Sobczak, K., Reorowicz, P., Obidowski, D., & Jóźwik, K. (2022, November). Influence of Tip Speed Ratio on the efficiency of Savonius wind turbine with deformable blades. In Journal of Physics: Conference Series (Vol. 2367, No. 1, p. 012003). IOP Publishing.

[17] Zakaria, A. (2020). Turbulence modelling of a helical Savonius wind turbine operating at low Reynolds number. CFD Letters, 12(5), 91-10.